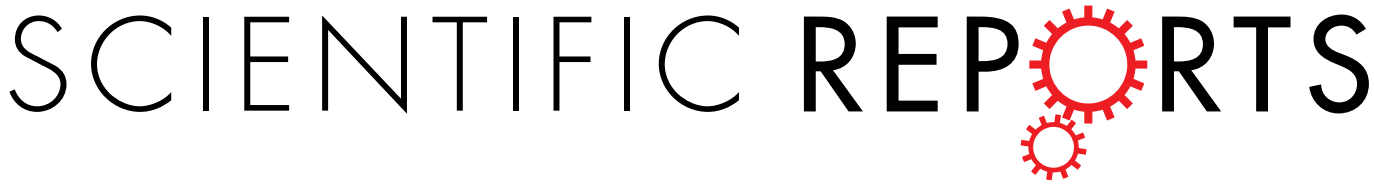

OPEN

Localization-delocalization wavepacket transition in Pythagorean aperiodic potentials

Received: 05 July 2016
Accepted: 11 August 2016
Published: 02 September 2016

Changming Huang[1,2], Fangwei Ye[1,2], Xianfeng Chen[1,2], Yaroslav V. Kartashov[3,4], Vladimir V. Konotop[5] & Lluis Torner[3,6]

We introduce a composite optical lattice created by two mutually rotated square patterns and allowing observation of continuous transformation between incommensurate and completely periodic structures upon variation of the rotation angle θ. Such lattices acquire periodicity only for rotation angles $\cos\theta = a/c$, $\sin\theta = b/c$, set by Pythagorean triples of natural numbers (a, b, c). While linear eigenmodes supported by lattices associated with Pythagorean triples are always extended, composite patterns generated for intermediate rotation angles allow observation of the localization-delocalization transition of eigenmodes upon modification of the relative strength of two sublattices forming the composite pattern. Sharp delocalization of supported modes for certain θ values can be used for visualization of Pythagorean triples. The effects predicted here are general and also take place in composite structures generated by two rotated hexagonal lattices.

The formation and evolution of localized excitations in inhomogeneous systems, governed by the Schrödinger equation[1], is of paramount importance for understanding a variety of fundamental physical phenomena. These include quantum particles in the external potentials, matter waves in traps[2–4], evolution of optical pulses[5] and beams[6]. The dynamics of such systems are determined by the properties of the corresponding potentials. Thus, periodic potentials support only delocalized Bloch waves in the allowed bands of the spectrum[7], while in disordered potentials all eigenmodes can be localized[8]. Yet another scenario is encountered in aperiodic potentials which, however, feature long-range order, such as fractals[9] or quasi-crystals[10–12]. Eigenmodes in one-dimensional (1D) aperiodic systems may exhibit localization-delocalization transition (LDT) upon smooth deformation of the underlying potential[13–19], a behavior that places them between periodic and fully disordered systems.

The fundamental relevance of aperiodic structures featuring long-range order became obvious after discovery of quasi-crystals[10] in experiments on electron diffraction[20]. Nowadays these and other types of aperiodic structures are widely studied in different areas of science[21,22]. Especially rich opportunities for experimentation with aperiodic structures appear in optics[23] and matter-waves[24], where quasi-crystal-like potentials can be induced by several interfering plane waves in reconfigurable geometries or fabricated in suitable materials[25,26].

The phenomenon of LDT was predicted upon analysis of the tight-binding model of incommensurable potentials[13] and in the framework of the Harper (alias Aubry-Andre) model[14–19], for which the existence of LDT was supplied by a mathematical proof[27]. In particular, wave localization in 1D quasi-crystals mediated by variation of their parameters was observed experimentally in optics[28,29] and in Bose-Einstein condensates[24]. LDT may also take place in dissipative incommensurable 1D lattices, obeying parity-time symmetry[30]. The existence of LDT in certain 1D aperiodic potentials, however, does not guarantee that the effect occurs in higher dimensions. Some experiments show diffraction in 2D aperiodic structures[11,12,31,32], while others[23,33–36] indicate the formation of localized modes.

[1]Department of Physics and Astronomy, Shanghai Jiao Tong University, Shanghai 200240, China. [2]Key Laboratory for Laser Plasma (Ministry of Education), IFSA Collaborative Innovation Center, Shanghai Jiao Tong University, Shanghai 200240, China. [3]ICFO-Institut de Ciencies Fotoniques, The Barcelona Institute of Science and Technology, 08860 Castelldefels (Barcelona), Spain. [4]Institute of Spectroscopy, Russian Academy of Sciences, Troitsk, Moscow Region, 142190, Russia. [5]Centro de Física Teórica e Computacional and Departamento de Física, Faculdade de Ciências, Universidade de Lisboa, Campo Grande 2, Edifício C8, Lisboa 1749-016, Portugal. [6]Universitat Politecnica de Catalunya, 08034, Barcelona, Spain. Correspondence and requests for materials should be addressed to F.Y. (email: fangweiye@sjtu.edu.cn)

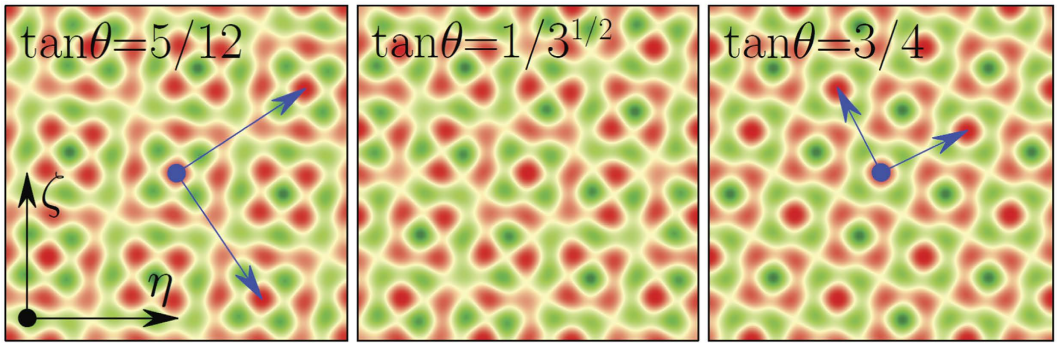

Figure 1. Lattices obtained by mutual rotation of two square lattices by an angle θ corresponding to the (5, 12, 13) and (3, 4, 5) triples (left and right panels, respectively) and of an aperiodic potential (central panel). The blue arrows show the primitive vectors. Lattices described by (1) are shown within the $\eta, \zeta \in [-4\pi, 4\pi]$ window for $p_1 = 1$ and $p_2 = 0.5$.

In this paper we introduce aperiodic potentials built as a superposition pattern of two identical periodic sublattices (either square or hexagonal) mutually-rotated by an angle θ. By changing θ the potential can be continuously transformed from periodic to aperiodic geometries and *vice versa*, without any change to its rotational point symmetry. The restoration of periodicity may occur at an infinite set of the rotation angles given by Pythagorean triples, at which the linear modes turn into Bloch waves. For hexagonal sublattices, we uncover new triples leading to periodicity restoration. Using such potentials we establish the existence of previously elusive 2D LDT. Furthermore, in our case LDT occurs not only upon variation of the relative depth of two sublattices, but also upon variation of the rotation angle. We show how the restoration of periodicity affects the thresholds for formation of self-sustained solitary waves previously studied only in quasi-crystals with predetermined symmetry[23,37–44]. The results obtained are directly applicable both in optics, where an aperiodic refractive index can be induced in various materials[45–49], and in Bose-Einstein condensates which can be manipulated by optical lattices[2–4]. In view of the recent interest in moiré patterns resulting from two superimposed honeycomb lattices with slightly different parameters, like graphene on hexagonal Boron Nitride(hBN)[50–53], we emphasize that the aperiodic structures reported are based on identical sublattices allowing restoration of periodicity upon change of the rotation angle.

Incommensurability is at the heart of construction of aperiodic potentials. It is also one of the most important objects in number theory, which has been in use since the time of the ancient Greeks[54]. The celebrated Pythagorean theorem is intimately related to incommensurability: it gives rise to so-called Pythagorean triples, i.e. natural numbers (a, b, c) satisfying the condition $a^2 + b^2 = c^2$ and setting lengths of catheti and hypotenuses of a right (Pythagorean) triangle. There are 16 primitive Pythagorean triples with $c < 100$, including (3, 4, 5), (5, 12, 13), (8, 15, 17), etc. These are directly connected with the transition between the fully periodic and aperiodic geometries introduced here. For example, consider a potential $V(\mathbf{r})$ [hereafter $\mathbf{r} = (\eta, \zeta)$ is a two-dimensional (2D) transverse position vector with η and ζ being spatial coordinates] created by two basic square lattices with equal periods that are mutually rotated by an angle of θ:

$$V(\mathbf{r}) = V_1(\mathbf{r}) + \frac{p_2}{p_1} V_1(S\mathbf{r}), \quad S = \begin{pmatrix} \cos\theta & -\sin\theta \\ \sin\theta & \cos\theta \end{pmatrix}, \tag{1}$$

where $V_1(\mathbf{r}) = p_1[\cos(2\eta) + \cos(2\zeta)]$ is one of the sub-lattices, and p_1 and p_2 are the sublattice depths. The potential (1) is aperiodic for all values of θ except when Pythagorean triangles are formed, i.e. when $\cos\theta = a/c$ and $\sin\theta = b/c$, where (a, b, c) is a Pythagorean triple. In this last case the periodicity of potential is restored[55]. Examples of such lattices – called Pythagorean lattices – are shown in Fig. 1. Each Pythagorean lattice possesses a square primitive cell (see ref. 55 for technical details), whose area depends on the Pythagorean triple defining it. For all other rotation angles the potential $V(\mathbf{r})$ exhibits an aperiodic structure with long-range order (shown in the central panel of Fig. 1). Therefore, variation of θ causes a smooth transformation between periodic and quasi-periodic structures, while the underlying four-fold rotation symmetry is *always preserved*. Modifications in the lattice depths p_1 and p_2 do not affect the four-fold lattice symmetry either, thereby making the potential (1) particularly convenient to study the occurrence of LDT phenomena.

We note that one standard approach to create optical quasi-crystals relies on the superposition of N plane waves, with N being odd and selected such that the pattern in principle cannot be periodic. In our case we use two sets of four plane waves that are mutually-rotated. Their superposition can give rise to a periodic distribution for certain rotation angles and to aperiodic distributions for all other angles (the possibility of generating quasi-crystals in the sense of the generally accepted definition[11,12] remains an open question).

Let us now consider a Pythagorean lattice as an optical potential for light propagation. In a paraxial approximation, a light beam with amplitude q in a medium with the shallow refractive index modulation (1) is governed by the dimensionless Schrödinger equation

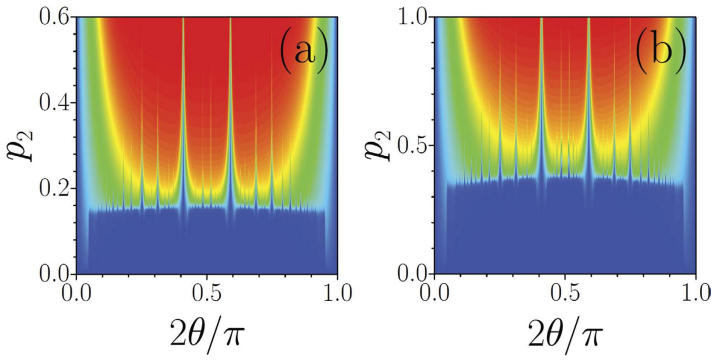

Figure 2. LDT illustrated by $\chi(\theta, p_2)$ dependencies for (**a**) $p_1 = 1$ and (**b**) $p_1 = 0.5$. Blue domains correspond to completely delocalized states and green/red domains correspond to localized modes.

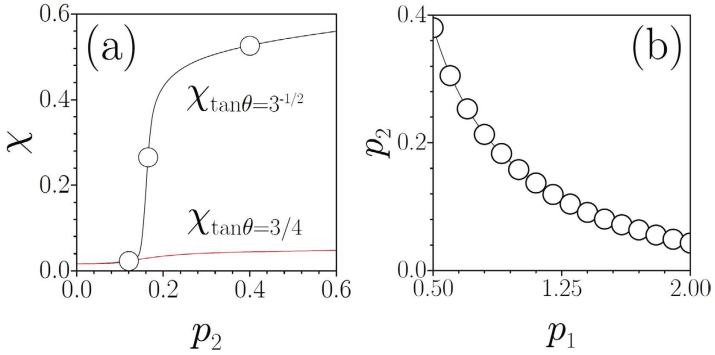

Figure 3. (**a**) Form-factor *vs* p_2 for periodic (red curve) and quasi-periodic (black curve) lattices at $p_1 = 1$. Circles correspond to linear modes from Fig. 4(a). (**b**) LDT threshold on (p_1, p_2)-plane defined as a line where $\chi = 0.1$ at $\theta = \pi/6$.

$$i\frac{\partial q}{\partial \xi} = -\frac{1}{2}\nabla^2 q - V(\mathbf{r})q + \sigma|q|^2 q, \tag{2}$$

which accounts for focusing (defocusing) Kerr nonlinearity at $\sigma = -1$ ($\sigma = +1$), and becomes linear at $\sigma = 0$. Here $\nabla \equiv (\partial/\partial\eta, \partial/\partial\zeta)$ and ξ is the propagation distance.

The eigenmodes of the linear system (i.e. when $\sigma = 0$) are searched for in the form $q(\eta, \zeta, \xi) = w(\eta, \zeta)e^{i\beta\xi}$, where the function $w(\eta, \zeta)$ describes the mode profile and β is its propagation constant. The degree of transverse localization of the modal field can be characterized by the integral form-factor $\chi = U^{-1}\left(\int |q|^4 d\mathbf{r}\right)^{1/2}$, where $U = \int |q|^2 d\mathbf{r}$ is the energy flow. The form-factor is inversely proportional to the mode width. Hence, higher χ means stronger localization.

One of our main results is illustrated in Figs 2 and 3. It consists of observation of the LDT in a 2D aperiodic structure created by two rotated square lattices. Figure 2 shows representative dependencies of the form-factor of the eigenmode with largest β on the rotation angle θ (here $\theta \in [0, \pi/2]$) and on the depth p_2 of the second lattice.

For a fixed p_1 a relatively sharp LDT occurs when p_2 exceeds certain critical value [see typical dependence $\chi(p_2)$ in Fig. 3(a) and associated transformation of mode profiles in Fig. 4(a) for the angle $\tan\theta = 3^{-1/2}$ corresponding to an aperiodic potential]. Since gradual transition from delocalized to strongly localized modes occurs within a narrow interval of p_2 values, we define the LDT threshold as a p_2 value at which form-factor χ exceeds 0.1. The LDT threshold depends on depths of both sublattices p_1, p_2 and not on their ratio, as is obvious from Fig. 3(b). The lesser the depth of one sub-lattice the deeper the other sub-lattice should be for the onset of localization. Surprisingly, however, the threshold depends very weakly on the rotation angle [see weakly varying boundary between blue and green/red domains in Fig. 2(a,b)].

When the rotation angle coincides with a Pythagorean angle the potential periodicity is restored and all modes become delocalized regardless of p_2 as they represent conventional Bloch states [see lower curve in Fig. 3(a)]. Such Pythagorean angles are clearly identified in Fig. 2 by the location of narrow vertical (blue) delocalization stripes. Thus, Pythagorean triples *can actually be visualized* by capturing the linear diffraction patterns produced by narrow inputs: even if p_2 is above the LDT threshold, a sudden delocalization of the output pattern occurs for rotation angles θ coinciding with any Pythagorean angle. This is shown in Fig. 4(b,c), which compare linear propagation of

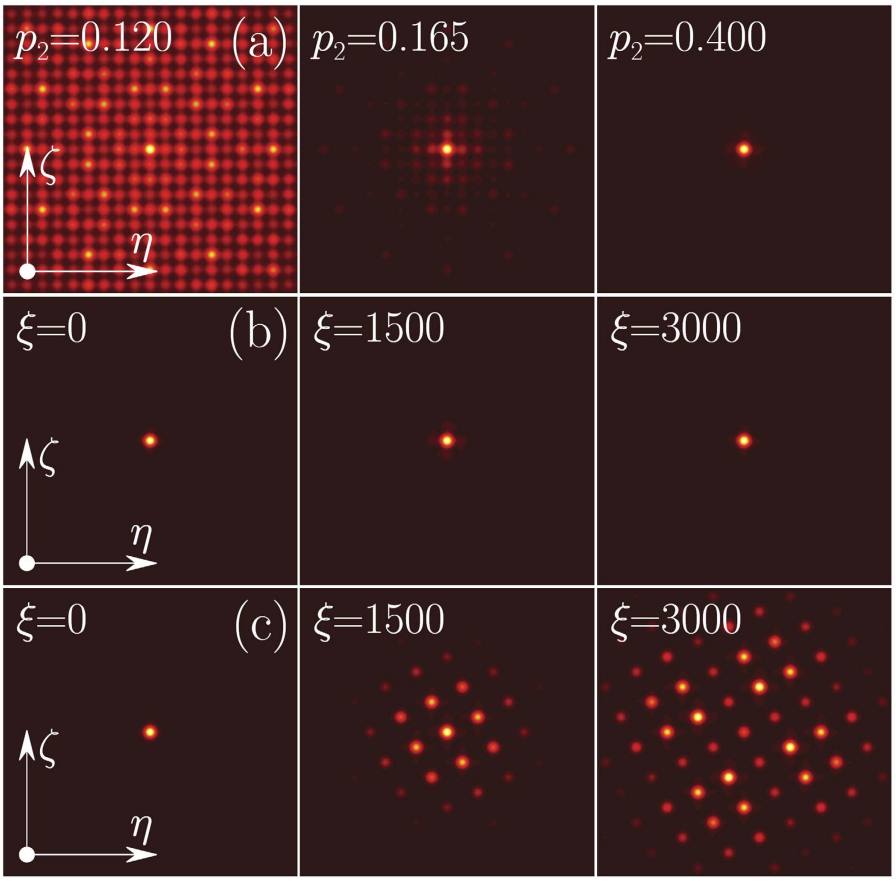

Figure 4. (**a**) Field modulus distributions in the linear mode with the largest propagation constant supported by the lattice with $\tan\theta = 3^{-1/2}$ and $p_1 = 1$ for different p_2. Field modulus distributions for a single-site input beam at three different distances in the aperiodic potential with $\tan\theta = 3^{-1/2}$ (**b**) and in the Pythagorean lattice with $\tan\theta = 3/4$ (**c**) at $p_1 = 1$ and $p_2 = 0.4$.

narrow Gaussian beams in aperiodic ($\tan\theta = 3^{-1/2}$) and Pythagorean ($\tan\theta = 3/4$) potentials. Note the four-fold rotation symmetry exhibited by the linear diffraction pattern in Fig. 4(c).

In Fig. 5(a) we show the band-gap spectrum of the Pythagorean lattice corresponding to $\tan\theta = 3/4$ [the triple (3, 4, 5)]. Note that the $\alpha = 1$ band is remarkably flat. Since the effective diffraction strength is determined by the band curvature, the flatness causes an anomalously slow broadening of the beam that excites modes from this flat band. Such effect, which was observed earlier in other lattice types[56–58], is also well observable in the Pythagorean lattice as seen in Fig. 4(c). Note that the input standard Gaussian beams that we use here excite mostly modes from the top flat band, while they do not excite modes from the lower bands that are not necessarily flat.

Returning to new possibilities afforded by the smooth one-parametric transition between periodic and aperiodic geometries, one may wonder what happens to the linear spectrum when the transition takes place. The answer is given in Fig. 5(b), which shows the evolution of 600 largest eigenvalues β_k of the system (corresponding modes are calculated on the $[-80\pi, +80\pi]$ window with zero boundary conditions) when the deviation of the rotation angle from a Pythagorean angle increases. The gap between the first and second groups of eigenvalues (former $\alpha = 1$ and $\alpha = 2$ bands) does not disappear abruptly and it only closes completely for deviations in θ of the order of 0.5 degrees. Therefore, phenomena associated with the presence of forbidden gaps can occur even in slightly aperiodic lattices. Thus, in a nonlinear system the persistence of a finite gap for the slight detuning of the rotation angle from a Pythagorean implies that the energy flow threshold for gap soliton existence does not disappear abruptly upon detuning.

The potential (1) also has an impact on the properties of nonlinear localized states. It has been proven[59] that in the focusing 2D nonlinear Schrödinger equation with a periodic potential, a minimal energy flow U is required to create a 2D soliton. This is applicable to model (2) with a Pythagorean lattice $V(\mathbf{r})$ and with $\sigma = -1$. On the other hand, if a system supports localized linear modes, one can expect that solitons may bifurcate from such modes with an increase of the peak amplitude. Thus, for periodic and aperiodic potentials one expects qualitatively different behavior of the $U(\beta)$ curves (here β is the propagation constant of soliton $q = w(\eta, \zeta)e^{i\beta\xi}$). This is confirmed by Fig. 6(a) for $\sigma = -1$. Indeed, for $\tan\theta = 3/4$ corresponding to periodic potential (black curves 1 and 2), a minimal energy flow is required for soliton formation irrespectively of p_2 value. However, for $\tan\theta = 3^{-1/2}$ the $U(\beta)$ curves are qualitatively different below (red curve 1) and above (red curve 2) LDT threshold in p_2: in the former case minimal energy flow is still needed to form a soliton, while in the latter case energy flow goes to zero

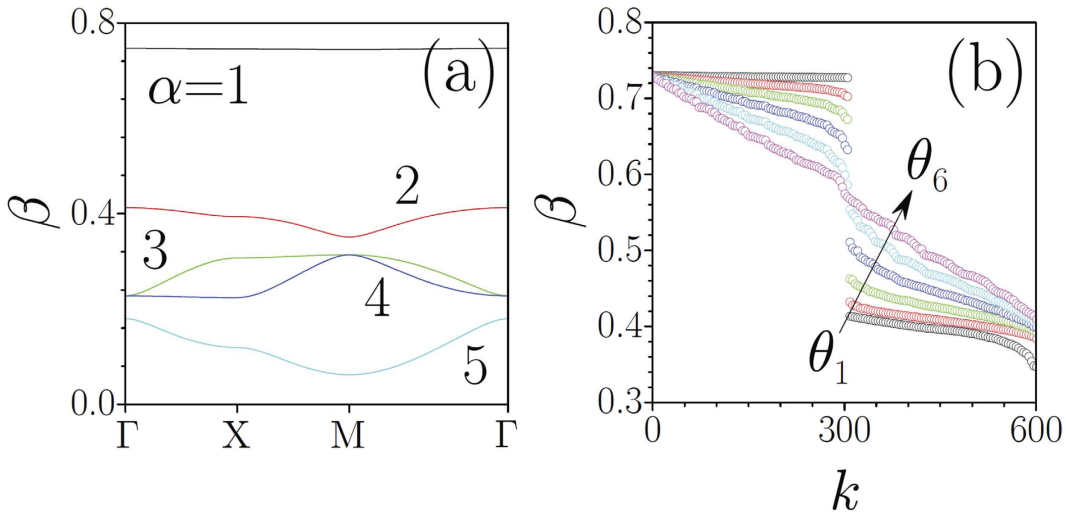

Figure 5. (**a**) Band-gap spectrum of a periodic lattice with $\tan\theta = 3/4$. (**b**) The transformation of discrete spectrum β_k of aperiodic lattice upon increase of the rotation angle from $\theta_1 = \arctan(3/4) + \pi/1800$ (black circles) to $\theta_6 = \arctan(3/4) + 6\pi/1800$ (magenta circles) in equal steps of $\pi/1800$. In both cases $p_1 = 1$, $p_2 = 0.4$.

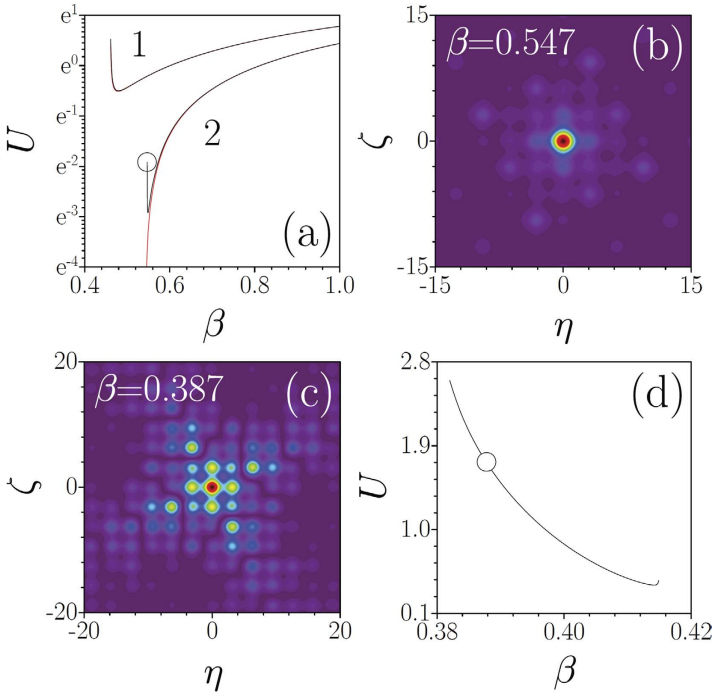

Figure 6. Energy flow *U vs* β for solitons in focusing media at $p_2 = 0.05$ (curve 1) and $p_2 = 0.22$ (curve 2). The black and red curves correspond to lattices with $\tan\theta = 3/4$ and $\tan\theta = 3^{-1/2}$. (**b**) Soliton corresponding to the circle in (**a**). (**c**) Gap solitons in defocusing media corresponding to the circle in (**d**). (**d**) $U(\beta)$ dependence for gap solitons in the lattice with $p_2 = 0.1$ and $\theta = \arctan(3/4) + \pi/900$. In all cases $p_1 = 1$. Panels (**b,c**) show field modulus distribution.

indicating a bifurcation from linear mode. Solitons are found to be stable for the intervals where $dU/d\beta > 0$[55], similarly to prediction of the Vakhitov-Kolokolov stability criterion. In a Pythagorean lattice with defocusing nonlinearity ($\sigma = +1$) solitons may form in finite gaps, even for a small detuning of the rotation angle from a Pythagorean one [see Fig. 6(d) for the corresponding $U(\beta)$ curve]. Such solitons feature an energy flow threshold and are stable in the largest part of the gap, except for narrow regions close to the gap edges. Note the unusual symmetry of the soliton shapes supported by the composite lattices [Fig. 6(b,c)].

The above results are general in the sense that the mutual rotation of two geometrically identical structures (of any symmetry) sets the basis for the construction of one-parametric 2D potentials allowing continuous transition between periodic and aperiodic geometries and, hence, observation of LDT. To illustrate the generality of

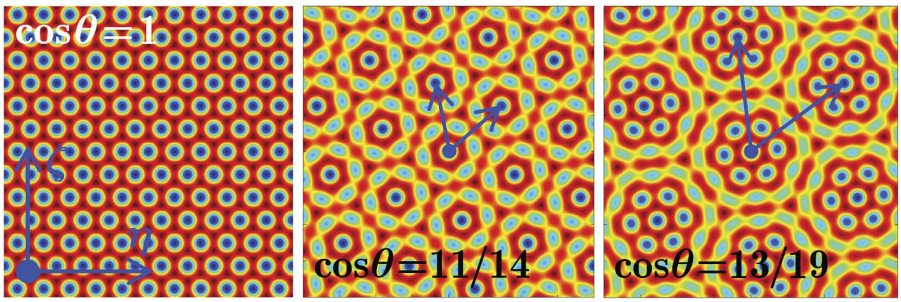

Figure 7. Potentials obtained mutual rotations of two hexagonal lattices for $\cos\theta = 1$ (left), $\cos\theta = 11/14$ (center) and $\cos\theta = 13/19$ (right). The lattices are shown within the $\eta, \zeta \in [-20, 20]$ window for $p_1 = p_2 = 1$. The blue arrows in the central and right panels are the primitive vectors.

the effect we consider the potential (1) composed of two rotated hexagonal (triangular) lattices $V_1(\mathbf{r}) = -\sum_{i=1,2,3} \cos[\Omega \cdot (\eta \cos\theta_i + \zeta \sin\theta_i)]$, where $\theta_i = 0, 2\pi/3, 4\pi/3$. Examples of such composite potentials are given in Fig. 7. By analogy with Pythagorean triples, it is possible to introduce a triple of positive integers (a, b, c), such that $c^2 = a^2 + b^2 + ab$, which uniquely defines the rotation angle (its tangent is given by $\tan\theta = b\sqrt{3}/(2a + b)$) at which periodicity is restored. Such triples are different from Pythagorean triples[55]. The corresponding lattices also feature LDT, while restoration of lattice periodicity for suitable rotation angles leads to delocalization depths in the $\pi/3$-periodic $\chi(\theta)$ dependencies qualitatively similar to those encountered in square rotated lattices[55].

Conclusions

In summary, we have shown that LDT can occur in a new class of *two-dimensional* composite lattices created by the superposition of two mutually-rotated periodic structures. Even above the LDT threshold for given amplitudes of the sub-lattices, where all eigenmodes are localized for the majority of rotation angles, one observes *sharp delocalization* for rotation angles corresponding to Pythagorean triples. Thus, for specific rotation angles θ allowing periodicity restoration one always gets delocalization, while for θ values leading to aperiodic lattices localization occurs for p_1, p_2 values taken above the LDT threshold. Since this conclusion is based on general arguments we anticipate that the localization-delocalization transition can be observed in structures with different internal symmetries and can be experimentally realized in various systems, including optical settings and Bose-Einstein condensates. The nature of the underlying composite linear lattices also has an impact on the properties and symmetries of nonlinear self-sustained excitations, allowing, for example, thresholdless creation of *two-dimensional* solitons in media with Kerr nonlinearity.

References

1. Schrödinger, E. An undulatory theory of the mechanics of atoms and molecules. *Phys. Rev.* **28,** 1049 (1926).
2. Dalfovo, F., Giorgini, S., Pitaevskii, L. P. & Stringari, S. Theory of Bose-Einstein condensation in trapped gases. *Rev. Mod. Phys.* **71,** 463 (1999).
3. Brazhnyi, V. A. & Konotop, V. V. Theory of nonlinear matter waves in optical lattices. *Mod. Phys. Lett. B* **18,** 627–651 (2004).
4. Morsch, O. & Oberthaler, M. Dynamics of Bose-Einstein condensates in optical lattices. *Rev. Mod. Phys.* **78,** 179 (2006).
5. Agrawal, G. P. *Nonlinear fiber optics*. (Academic press, 2007).
6. Kivshar, Y. S. & Agrawal, G. *Optical solitons: from fibers to photonic crystals*. (Academic press, 2003).
7. Bloch, F. Über die quantenmechanik der elektronen in kristallgittern. *Z. Phys* **52,** 555–600 (1929).
8. Anderson, P. W. Absence of diffusion in certain random lattices. *Phys. Rev.* **109,** 1492 (1958).
9. Mandelbrot, B. B. *The fractal geometry of nature*. Vol. 173 (Macmillan, 1983).
10. Levine, D. & Steinhardt, P. Quasicrystals: A new class of ordered structures. *Phys. Rev. Lett.* **53,** 2477 (1984).
11. Janot, C. *Quasicrystals: A Primer*. (Clarendon Press, Oxford, 1994).
12. Dal Negro, L. & Boriskina, S. V. Deterministic aperiodic nanostructures for photonics and plasmonics applications. *Laser Photonics Rev*. **6,** 178–218 (2012).
13. Soukoulis, C. M. & Economou, E. N. Localization in one-dimensional lattices in the presence of incommensurate potentials. *Phys. Rev. Lett.* **48,** 1043 (1982).
14. Harper, P. G. Single band motion of conduction electrons in a uniform magnetic field. *Proc. Phys. Soc., Sect. A* **68,** 874 (1955).
15. Aubry, S. & André, G. Analyticity breaking and Anderson localization in incommensurate lattices. *Ann. Israel Phys. Soc* **3,** 18 (1980).
16. Thouless, D. J. Bandwidths for a quasiperiodic tight-binding model. *Phys. Rev. B* **28,** 4272 (1983).
17. Grempel, D. J., Fishman, S. & Prange, R. E. Localization in an incommensurate potential: An exactly solvable model. *Phys. Rev. Lett.* **49,** 833 (1982).
18. Kohmoto, M. Metal-insulator transition and scaling for incommensurate systems. *Phys. Rev. Lett.* **51,** 1198 (1983).
19. Aulbach, C., Wobst, A., Ingold, G.-L., Hänggi, P. & Varga, I. Phase-space visualization of a metal–insulator transition. *New J. Phys.* **6,** 70 (2004).
20. Shechtman, D., Blech, I., Gratias, D. & Cahn, J. W. Metallic phase with long-range orientational order and no translational symmetry. *Phys. Rev. Lett.* **53,** 1951 (1984).
21. Steurer, W. & Sutter-Widmer, D. Photonic and phononic quasicrystals. *J. Phys. D: Appl. Phys.* **40,** R229 (2007).
22. Vardeny, Z. V., Nahata, A. & Agrawal, A. Optics of photonic quasicrystals. *Nat. Photonics* **7,** 177–187 (2013).
23. Freedman, B. *et al.* Wave and defect dynamics in nonlinear photonic quasicrystals. *Nature* **440,** 1166–1169 (2006).
24. Roati, G. *et al.* Anderson localization of a non-interacting Bose–Einstein condensate. *Nature* **453,** 895–898 (2008).
25. Kaliteevski, M. A. *et al.* Two-dimensional Penrose-tiled photonic quasicrystals: from diffraction pattern to band structure. *Nanotechnology* **11,** 274 (2000).

26. Chan, Y., Chan, C. T. & Liu, Z. Y. Photonic band gaps in two dimensional photonic quasicrystals. *Phys. Rev. Lett.* **80,** 956 (1998).
27. Jitomirskaya, S. Y. Metal-insulator transition for the almost Mathieu operator. *Ann. Math.* **150,** 1159–1175 (1999).
28. Lahini, Y. *et al.* Observation of a localization transition in quasiperiodic photonic lattices. *Phys. Rev. Lett.* **103,** 013901 (2009).
29. Gellermann, W., Kohmoto, M., Sutherland, B. & Taylor, P. Localization of light waves in Fibonacci dielectric multilayers. *Phys. Rev. Lett.* **72,** 633 (1994).
30. Hang, C., Kartashov, Y. V., Huang, G. & Konotop, V. V. Localization of light in a parity-time-symmetric quasi-periodic lattice. *Opt. Lett.* **40,** 2758–2761 (2015).
31. Allain, C. & Cloitre, M. Optical diffraction on fractals. *Phys. Rev. B* **33,** 3566 (1986).
32. Allain, C. & Cloitre, M. Spatial spectrum of a general family of self-similar arrays. *Phys. Rev. A* **36,** 5751 (1987).
33. Della Villa, A. *et al.* Localized modes in photonic quasicrystals with Penrose-type lattice. *Opt. Express* **14,** 10021–10027 (2006).
34. Levi, L. *et al.* Disorder-enhanced transport in photonic quasicrystals. *Science* **332,** 1541–1544 (2011).
35. Mnaymneh, K. & Gauthier, R. C. Mode localization and band-gap formation in defect-free photonic quasicrystals. *Opt. Express* **15,** 5089–5099 (2007).
36. Dong, J.-W., Fung, K. H., Chan, C. & Wang, H.-Z. Localization characteristics of two-dimensional quasicrystals consisting of metal nanoparticles. *Phys. Rev. B* **80,** 155118 (2009).
37. Johansson, M. & Riklund, R. Solitonlike states in a one-dimensional nonlinear Schrödinger equation with a deterministic aperiodic potential. *Phys. Rev. B* **49,** 6587 (1994).
38. Lindquist, B., Johansson, M. & Riklund, R. Soliton dynamics and interaction in a deterministic aperiodic nonlinear lattice. *Phys. Rev. B* **50,** 9860 (1994).
39. Xie, P., Zhang, Z.-Q. & Zhang, X. Gap solitons and soliton trains in finite-sized two-dimensional periodic and quasiperiodic photonic crystals. *Phys. Rev. E* **67,** 026607 (2003).
40. Saḳaguchi, H. & Malomed, B. A. Gap solitons in quasiperiodic optical lattices. *Phys. Rev. E* **74,** 026601 (2006).
41. Ablowitz, M. J., Ilan, B., Schonbrun, E. & Piestun, R. Solitons in two-dimensional lattices possessing defects, dislocations, and quasicrystal structures. *Phys. Rev. E* **74,** 035601 (2006).
42. Ablowitz, M. J., Antar, N., Bakirtaş, İ. & Ilan, B. Band-gap boundaries and fundamental solitons in complex two-dimensional nonlinear lattices. *Phys. Rev. A* **81,** 033834 (2010).
43. Law, K. J. H., Saxena, A., Kevrekidis, P. G. & Bishop, A. R. Stable structures with high topological charge in nonlinear photonic quasicrystals. *Phys. Rev. A* **82,** 035802 (2010).
44. Ablowitz, M. J., Antar, N., Bakirtaş, İ. & Ilan, B. Vortex and dipole solitons in complex two-dimensional nonlinear lattices. *Phys. Rev. A* **86,** 033804 (2012).
45. Gauthier, R. C. & Mnaymneh, K. W. Design of photonic band gap structures through a dual-beam multiple exposure technique. *Opt. Laser Technol.* **36,** 625–633 (2004).
46. Boguslawski, M., Rose, P. & Denz, C. Increasing the structural variety of discrete nondiffracting wave fields. *Phys. Rev. A* **84,** 013832 (2011).
47. Jin, W. & Gao, Y. Optically induced two-dimensional photonic quasicrystal lattices in iron-doped lithium niobate crystal with an amplitude mask. *Appl. Phys. Lett.* **101,** 141104 (2012).
48. Kraus, Y. E., Lahini, Y., Ringel, Z., Verbin, M. & Zilberberg, O. Topological states and adiabatic pumping in quasicrystals. *Phys. Rev. Lett.* **109,** 106402 (2012).
49. Rose, P., Boguslawski, M. & Denz, C. Nonlinear lattice structures based on families of complex nondiffracting beams. *New J. Phys.* **14,** 033018 (2012).
50. Decker, R. *et al.* Local electronic properties of graphene on a BN substrate via scanning tunneling microscopy. *Nano Lett.* **11,** 2291–2295 (2011).
51. Woods, C. *et al.* Commensurate-incommensurate transition in graphene on hexagonal boron nitride. *Nat. Phys.* **10,** 451–456 (2014).
52. Ni, G. *et al.* Plasmons in graphene moire superlattices. *Nat. Mater.* **14,** 1217 (2015).
53. Wang, D. *et al.* Thermally Induced Graphene Rotation on Hexagonal Boron Nitride. *Phys. Rev. Lett.* **116,** 126101 (2016).
54. According to some sources [von Fritz, K. The Discovery of Incommensurability by Hippasus of Metapontum. *Ann. Math.* **46,** 242 (1945)] the discovery of incommensurability can be attributed to Hippasus of Metapontum.
55. The elementary properties of the Pythagorean and composite hexagonal lattices, as well as propagation dynamics of solitions are described in the Supplemental Material.
56. Yulin, A. V. & Konotop, V. V. Conservative and PT-symmetric compactons in waveguide networks. *Opt. Lett.* **38,** 4880–4883 (2013).
57. Leykam, D., Flach, S., Bahat-Treidel, O. & Desyatnikov, A. S. Flat band states: Disorder and nonlinearity. *Phys. Rev. B* **88,** 224203 (2013).
58. Flach, S., Leykam, D., Bodyfelt, J. D., Matthies, P. & Desyatnikov, A. S. Detangling flat bands into Fano lattices. *EPL (Europhys. Lett.)* **105,** 30001 (2014).
59. Ilan, B. & Weinstein, M. I. Band-edge solitons, nonlinear Schrödinger/Gross-Pitaevskii equations, and effective media. *Multiscale Model. Simul.* **8,** 1055–1101 (2010).

Acknowledgements

The work of C. Huang and F. Ye was supported by Innovation Program of Shanghai Municipal Education Commission (Grant No. 13ZZ022) and the National Natural Science Foundation of China (Grant No. 61475101). F. Ye also acknowledges the support from Doctoral Program Foundation of Institutions of Higher Education of China(20110073120074). V. V. Konotop acknowledges the support of the FCT (Portugal) grant UID/FIS/00618/2013. The work of Y. Kartashov and L. Torner has been partially supported by the Severo Ochoa Excellence program and Fundacio Cellex.

Author Contributions

All authors have made substantial contributions to the research work. Y.V.K. formulated the idea of two-dimensional LDT transition. V.V.K. suggested the Pythagorean lattices and performed analytical studies of their properties. C.H. performed the numerical simulations under supervision of F.Y. and X.C. Figures in the main text were prepared by Y.V.K. The main text was written by F.Y., Y.V.K., V.V.K. and L.T. The Supplementary Material was written by V.V.K., F.Y. and Y.V.K. All authors contributed to discussion of the results and to the revision of the manuscript.

Additional Information

Supplementary information accompanies this paper at http://www.nature.com/srep

Competing financial interests: The authors declare no competing financial interests.

How to cite this article: Huang, C. *et al.* Localization-delocalization wavepacket transition in Pythagorean aperiodic potentials. *Sci. Rep.* **6**, 32546; doi: 10.1038/srep32546 (2016).